A bioinspired approach to engineer seed microenvironment to boost germination and mitigate soil salinity

Augustine T. Zvinavashe[a], Eugene Lim[a], Hui Sun[a], and Benedetto Marelli[a,1]

[a]Department of Civil and Environmental Engineering, Massachusetts Institute of Technology, Cambridge, MA 02139

Edited by Jeffery L. Dangl, University of North Carolina, Chapel Hill, NC, and approved October 31, 2019 (received for review September 13, 2019)

Human population growth, soil degradation, and agrochemical misuse are significant challenges that agriculture must face in the upcoming decades as it pertains to global food production. Seed enhancement technologies will play a pivotal role in supporting food security by enabling germination of seeds in degraded environments, reducing seed germination time, and boosting crop yields. So far, a great effort has been pursued in designing plants that can adapt to different environments and germinate in the presence of abiotic stressors, such as soil salinity, heat, and drought. The technology proposed here seeks a different goal: To engineer the microenvironment of seeds by encapsulation, preservation, and precise delivery of biofertilizers that can boost seed germination and mitigate abiotic stressors. In particular, we developed a biomaterial based on silk fibroin (S) and trehalose that can be mixed with rhizobacteria and applied on the surface of seeds, retrofitting currently used techniques for seed coating, i.e., dip coating or spray drying. A micrometer thick transparent robust coating is formed by material assembly. The combination of a polymorphic protein as S and of a disaccharide used by living systems to tolerate abiotic stressors provides a beneficial environment for the survival of nonspore forming rhizobacteria outside the soil and in anhydrous conditions. Using *Rhizobium tropici* CIAT 899 and *Phaseolus vulgaris* as working models, we demonstrated that rhizobacteria delivered in the soil after coating dissolution infect seedlings' roots, form root nodules, enhance yield, boost germination, and mitigate soil salinity.

seed | trehalose | silk | rhizobia | coating

Global food production is projected to rise in the upcoming decades due to 800 million people currently lacking food security and 9.7 billion people projected to inhabit the world by 2050 (1). Land degradation, excessive freshwater consumption, and misuse of agrochemicals cause inefficiencies in agricultural practices, while changes in climate patterns and spread of transboundary pests and diseases require rapid crop adaptation to abiotic and biotic stresses. To address these challenges, precision agriculture has emerged based on advanced technologies designed to make food production more efficient with the main goal of increasing crop production while minimizing inputs, such as water and agrochemicals and mitigating environmental impact (2–4). As a result, agriculture is becoming more sustainable and technologically driven with big data analysis, geolocalization, modernization of mechanical equipment, and sensing systems being the main drivers of innovation in a sector that, in recent years, has mostly benefited from improvements in agrochemical formulations, weather prediction, breeding, and seed engineering.

Seeds are the agricultural product with the most value added and not only represent a source of food, but also represent the most important resource in agricultural practices (5). There are many reasons for seedling suboptimal germination and mortality including diseases, pests, excessive use of fertilizers in the seed row, improper seeding depth, osmotic stress, frost, and drought (6). The use of precision tools to manage seed sowing and to support germination is then paramount to guarantee efficiency in terms of output over space. In the past few years, seed enhancement technologies have emerged to improve seed performance by exposure to specific conditioning and regimes (7). Seed coatings have been developed to control seed surface properties, locally enrich the soil with nutrients, and influence seed water uptake (5, 8). However, the attention has mostly been focused on the investigation of payloads used to boost seed germination as a function of soil properties and seed type rather than on the materials used to encapsulate and deliver the payloads. This approach has limited the formulation of seed coatings that encapsulate beneficial but labile compounds, such as biofertilizers, i.e., PGPRs that increase availability of nutrients and phytohormones during interaction with plant roots while mitigating the environmental side effects of synthetic fertilizers and pesticides (9–11). The incorporation of inocula in an artificial seed coat can result in the loss of microbial viability with coated seeds unable to be stored for extended periods of time (12). The synthetic seed coat is usually a hostile environment for PGPRs, mostly due to osmotic and desiccation stress and, when protectant compounds are present, their biological activity could pose a threat to the survival of symbiotic bacteria. Biomaterials that are adopted from the field of drug delivery represent a technological opportunity to develop an advanced seed-coating

Significance

In a world that strives to accommodate population growth and climate pattern changes, there is a compelling need to develop new technologies to enhance agricultural output while minimizing inputs and mitigating their effects on the environment. In this study, we describe a biomaterial-based approach to engineer the microenvironment of seeds through the preservation and delivery of plant growth promoting rhizobacteria (PGPRs) that are able to fix nitrogen and mitigate soil salinity. PGPRs are encapsulated in silk–trehalose (ST) coatings that achieve bacterial preservation and delivery upon sowing. The biomaterial choice is inspired by a recent finding that a combination of proteins and disaccharides is key for anhydrobiosis. This simple technology is effective to boost seed germination and mitigate soil salinity.

Author contributions: A.T.Z., E.L., H.S., and B.M. designed research; A.T.Z. and H.S. performed research; A.T.Z., E.L., H.S., and B.M. analyzed data; and A.T.Z., E.L., H.S., and B.M. wrote the paper.

Competing interest statement: A patent application that includes the technology reported in this manuscript has been filed through the Technology Licensing Office of the Massachusetts Institute of Technology. B.M. has a financial interest in Cambridge Crops, Inc., which uses S-based coatings to extend food shelf-life.

This article is a PNAS Direct Submission.

[1]To whom correspondence may be addressed. Email: Bmarelli@mit.edu.

This article contains supporting information online at https://www.pnas.org/lookup/suppl/doi:10.1073/pnas.1915902116/-/DCSupplemental.

First published November 27, 2019.

technology that combines biodegradation with encapsulation, preservation, and controlled release of payloads that can boost seed germination and mitigate stressors.

In this study, we developed a biomaterial-based approach to engineer seed coatings that can boost germination and mitigate abiotic stressors, such as soil salinity. In particular, we designed a biomaterial based on S extracted from *Bombyx mori* cocoons and trehalose. The mixture can be mixed with rhizobacteria and applied on the surface of seeds, retrofitting currently used techniques for seed coating, such as dip coating or spray drying. S is a structural protein that is well known for its application in textiles and that has been reinvented as a naturally derived technical material with applications in regenerative medicine, drug delivery, implantable optoelectronics, and food coating (13, 14). The structural protein is purified from cocoons into a water suspension using a water-based process that uses chaotropic agents as LiBr to break the inter- and intramolecular hydrogen bonds that cross-link S molecules into fibers (15). Upon removal of the ions via dialysis, S has the form of nanomicelles in water suspension that are stable for a period of time that ranges from days to months, depending on concentration, pH, and molecular weight (16, 17). Material assembly is driven by water removal and formation of new intra- and intermolecular hydrogen bonds. This process can be engineered to obtain several materials formats, including transparent robust membranes that have been used to extend the shelf life of perishable crops (18). The combination of a diblock copolymerlike structure with hydrophobic repetitive amino acid sequences spaced out by hydrophilic negatively charged nonrepetitive sequences make S polymorphic as the protein can be obtained in random coil or β-sheet rich structures, enabling the fabrication of silk materials that are water soluble or water insoluble, respectively (19, 20). The S structure also provides a distinct environment that can preserve labile compounds ranging from antibiotics to growth factors, enzymes, and viruses by mitigating oxidative stress, providing sufficient hydration, and maintaining biomolecules configuration in anhydrous conditions (21). Trehalose is a nonreducing disaccharide in which the 2 glucose units are linked via an α,α-(1, 1)-glycosidic bond. This disaccharide has been isolated from all domains of life including plants, animals, fungi, yeast, archaea, and bacteria (22). Trehalose is also industrially produced as it is used in the food, cosmetics, and pharmaceutical industries. This disaccharide can serve as a signaling molecule, as a reserve carbohydrate, and as a stress protectant (e.g., drought, cold, and salt stress) (23). Accumulation of trehalose occurs both intra- and extracellularly (22, 24, 25). There are 2 competing, but not mutually exclusive, hypotheses about the mechanism of trehalose-driven cellular protection; (i) the vitrification hypothesis suggests that trehalose forms a glasslike matrix within cells, physically preventing protein denaturation, protein aggregation, and membrane fusion, (ii) the water replacement hypothesis posits that hydrogen bonds between water and cellular components are replaced by trehalose as cells dry, which would also prevent protein denaturation, aggregation, and membrane fusion (26). Recently, it has been shown that a particular class of proteins known as intrinsically disordered proteins also contributes to anhydrobiosis. For example, a mixture of water-soluble proteins rich in hydrogen bonds and disaccharides is a successful strategy that anhydrobiotic organisms, such as tardigrades have developed to survive desiccation (27). Inspired by these recent findings, we have investigated a biomaterial formulation that synergistically use the coating-forming, payload encapsulation, preservation, and biodegradation capabilities of S with the ability of trehalose to offer protection from osmotic and desiccation stresses in rhizobacteria to develop a seed-coating technology that can boost germination and mitigate abiotic stressors, such as soil salinity.

Formulation of ST Biomaterials. Li et al. (28) have recently reported how the preservation of biomolecules in S formulations correlates with matrix β-relaxation as it does in sugar-based dry formulations. It was also found that inclusion of sugars, such as sucrose in S-based materials enhances the protein stabilizing performance as they can act as antiplasticizers that suppress β-relaxation and decelerate degradation rates. In Fig. 1, we report the effects of trehalose on S matrices. Molecular dynamic simulations were used to investigate the molecular mobility of a S-like system made by 18 $(GAGSGA)_2$ peptides organized in a β-sheet configuration when suspended in water or in a water–trehalose mixture (Fig. 1*A*). Time evaluation of the RMSD of the atomic position from the original conformation indicated that trehalose reduces the dynamics of the 18 peptide systems and correlates with the general knowledge that sugars form a matrix around proteins that lock them in the original conformation by slowing down protein dynamics. Experimentally, we have demonstrated that trehalose does not interfere with S assembly as its addition to S suspensions does not impart any modification to the random coil structure assumed by S nor does it drive protein assembly. Circular dichroism (CD) spectra of S and ST water suspensions depicted that the protein maintained a random coil structure (indicated by the negative bands near 195 nm and low ellipticity above 210 nm) (29) when exposed to increasing concentrations of trehalose, up to 75 dry wt% (Fig. 1*B*). Dynamic light scattering (DLS) was used to measure the hydrodynamic radius of S nanomicelles in S and ST water suspensions (Fig. 1*C*). No statistically significant difference ($P > 0.05$) was found in the measured nanomicelles diameters at increasing trehalose concentrations, indicating that trehalose does not influence the assembly of S molecules in water. Attenuated total reflection–FTIR (ATR–FTIR) was used to evaluate the effects of trehalose on S polymorphism upon drying (Fig. 1*D*). All of the spectra of S films obtained using an increasing concentration of trehalose had an amide I resonance centered at 1,647 cm^{-1}, indicating that the structure of S molecules was not affected by trehalose and possessed a random coil configuration (30). Interestingly, methods, such as water annealing that are commonly used to drive the random coil to β-sheet transition in assembled S molecules were still effective in crystallizing S at high concentrations of trehalose. This phenomenon suggests that the replacement of hydrogen bonds between S molecules and water with inter- and intramolecular hydrogen bonds may be thermodynamically favorable even in the presence of trehalose and that the protein can undergo structural reconfiguration, water loss, and volume change despite the trehalose-induced vitrification of the protein. Nanoindentation mechanical tests conducted on S films containing increasing concentrations of trehalose showed that films' hardness and Young's modulus increased as the trehalose concentration increased. The inclusion of large quantities (up to 75 wt%) of the disaccharide imparted an antiplasticizing effect, which followed the rule of mixture and resulted in a more brittle final material, especially at trehalose concentrations >50 dry wt% (Fig. 1*E*). However, when water annealing postprocessing was applied to enhance films' β-sheets content, the hardness and Young's modulus of ST materials did not follow the rule of mixture. Hardness increased for trehalose concentrations up to 25 dry wt% [i.e., ST(3:1)] and then decreased in films with a trehalose content of 50 and 75 dry wt% [i.e., ST(1:1) and ST(1:3), respectively]. Young's modulus of ST materials increased for ST(3:1) films and then plateaued for larger trehalose contents. In *SI Appendix*, Fig. S1, we report the characterization of films obtained by mixing S with sucrose, a disaccharide that was not considered in this study for seed-coating applications given its large use as a food ingredient. CD, DLS, and ATR-FTIR analyses showed that sucrose did not modify S folding and assembly behavior, similar to what found for trehalose (*SI Appendix*, Fig. S1 *A–D*). However, nanoindentation measurements showed that the rule of mixture can predict mechanical properties when sucrose is incorporated in S materials, even when water annealing is applied. These data suggest a difference in the effects of vitrification imparted by trehalose

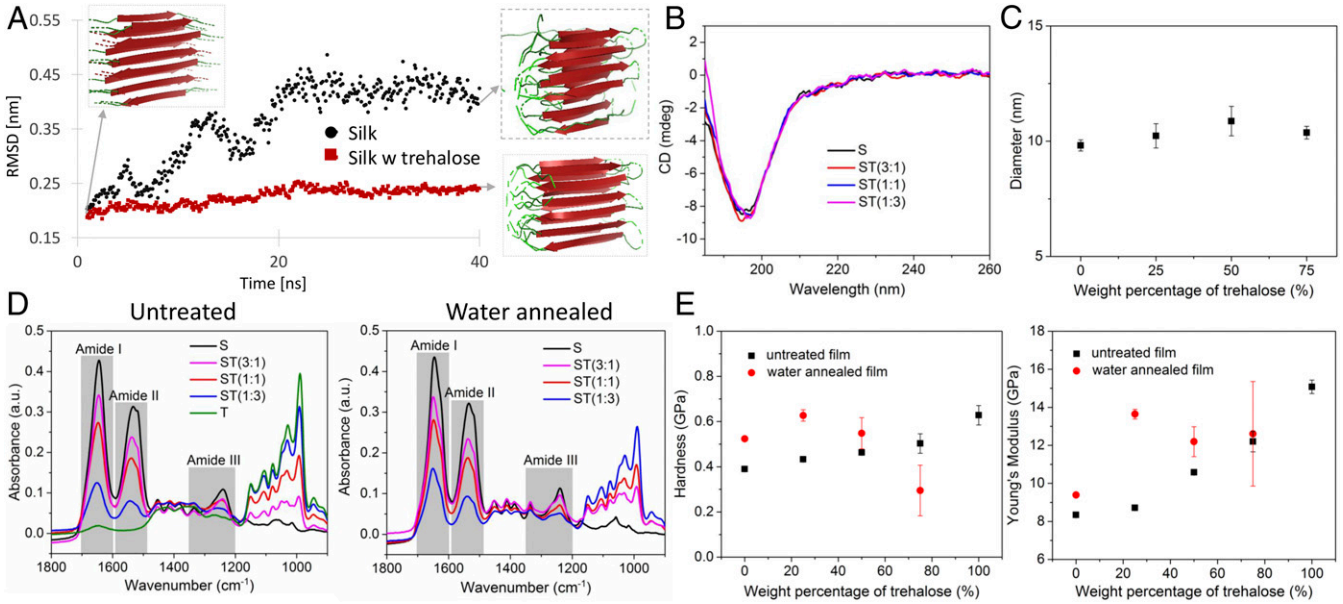

Fig. 1. Characterization of S, trehalose, and their mixtures used to manufacture films for seed coating. (*A*) Molecular dynamics simulation of S when exposed to water (black dots) and to a water and trehalose solvent matrix (red dots); root-mean-squared deviation (RMSD) measures average distance between the atoms. The 3 insets depict S structure after relaxation and at the end of the simulation (40 ns) in the different media. (*B*) Circular dichroism (CD) of suspensions of S and mixtures of S and ST. The disaccharide has no impact on the protein random coil conformation in water suspension as indicated by the negative bands near 195 nm and low ellipticity above 210 nm. (*C*) Dynamic light scattering (DLS) analysis of S nanomicelles aggregation in water as a function of trehalose concentration. The average diameter of silk nanomicelles was not affected by trehalose concentration in the water suspension. Error bars indicate SD. (*D*) Fourier transform infrared spectroscopy (FTIR) spectra of films obtained by drop casting of S, trehalose (T), and their mixtures (ST). The random coil-dominated resonance peaks of the amide bonds in the amide I and amide III regions were not affected by the presence of trehalose, indicating that the disaccharide has no effects on the protein polymorphism during the sol–gel-solid transition. In the *Right*, FTIR spectra show that a polymorphic random coil to β-sheet transition of S can be induced post film formation with water annealing as evidenced by the appearance of a peak at 1,621 cm^{-1}. (*E*) Mechanical properties of films consisting of S, trehalose, and their mixtures investigated with nanoindentation. Trehalose concentration and water-annealing postprocess resulted in an increase in hardness and apparent modulus and in the formation of more brittle films. Error bars indicate SD.

and sucrose on silk materials; trehalose possesses higher glass transition temperature ($T_g \sim 393$ K) when compared to sucrose ($T_g \sim 348$ K) and can form a more homogenous network with proteins (26, 31). As a result, the trehalose brittle matrix is disrupted by S random coil to β-sheets structural changes during water annealing, yielding a weaker material for trehalose concentrations >25 dry wt%. Nonetheless, ST materials showed mechanical properties on the order of currently available seed coatings (Young's modulus of 10^{-1}–10^{1} GPa) (32).

Coating Assembly and Biofertilizer Encapsulation and Release Performance. S assembly is driven by water evaporation and results in a sol–gel-solid transition process that yields a transparent material. The resulting film has a roughness of a few nanometers (measured by atomic force microscopy on flat films) and a thickness that can be controlled by modifying solution rheological parameters (33). At constant solid matter content, inclusion of trehalose in S suspensions decreases solution viscosity (*SI Appendix*, Fig. S2), which, however, remains on the order of 10^{-3} Pa·s, thereby enabling the application of ST suspensions on complex geometries, such as spheroids by retrofitting existing technologies commonly used for seed coating. Contact angle (θ) measurements also showed that θ decreases at higher trehalose concentration, given the higher hydrophilicty of the disaccharide when compared to S (*SI Appendix*, Fig. S2). When using borosilicate glass beads with a diameter of 5 mm as a model for seeds, dip coating, and spray drying of ST solutions enabled the encapsulation and delivery of payloads, such as PGPRs via formation of micrometer thick coatings that biodegrade when exposed to water (Fig. 2). Given the transparency of silk materials, we used GFP-producing PGPRs, such as GFP-modified *R. tropici* CIAT 899 (GFP-CIAT 899) to evaluate the encapsulation, preservation, and delivery of rhizobacteria. CIAT 899 is a broad host-range rhizobial strain and the most successful symbiont of *P. vulgaris* (34, 35). CIAT 899 provides high tolerance to environmental stresses, such as high temperature, acidity, and salinity, and its potential use as a biofertilizer is highly desirable but hindered by the low survivability of gram-negative bacteria during the desiccation and rehydration steps required for coating formation and inoculation (12, 36). In Fig. 2*A*, we report fluorescent images of glass beads coated with ST materials using dip-coating and spray drying techniques. When compared with the negative controls, it is possible to see how the GFP-CIAT 899 was successfully encapsulated in the coating materials as glass beads fluoresced when excited with a blue light. Spray-coated beads exhibited brighter fluorescence, which suggests the achievement of an enhanced encapsulation of GFP-CIAT 899. However, dip-coating methods are often preferable due to the easier implementation at scale. SEM was used to evaluate the thickness of the coatings obtained as a function of increasing relative concentration of trehalose in S matrices (i.e., dry mass remained constant). SEM micrographs revealed that coatings thickness was on the order of a few micrometers (5 ± 2 μm) and depicted the presence of bacteria in the vitrified polymer matrix (Fig. 2*B*). Successful encapsulation and release of GFP-CIAT 899 on glass beads as a function of ST mixture-coating material (i.e., increasing the relative content of trehalose) was then evaluated via streaking of resuscitated bacteria on an agar plate using a colony counting method (Fig. 2*C*). Given the coating thickness (t), the spherical geometry of the substrate (r), the known concentration of bacteria in the coating solution (C_b), and assuming a homogenous dispersion of bacteria and the formation of a homogenous coating, it is possible to estimate the

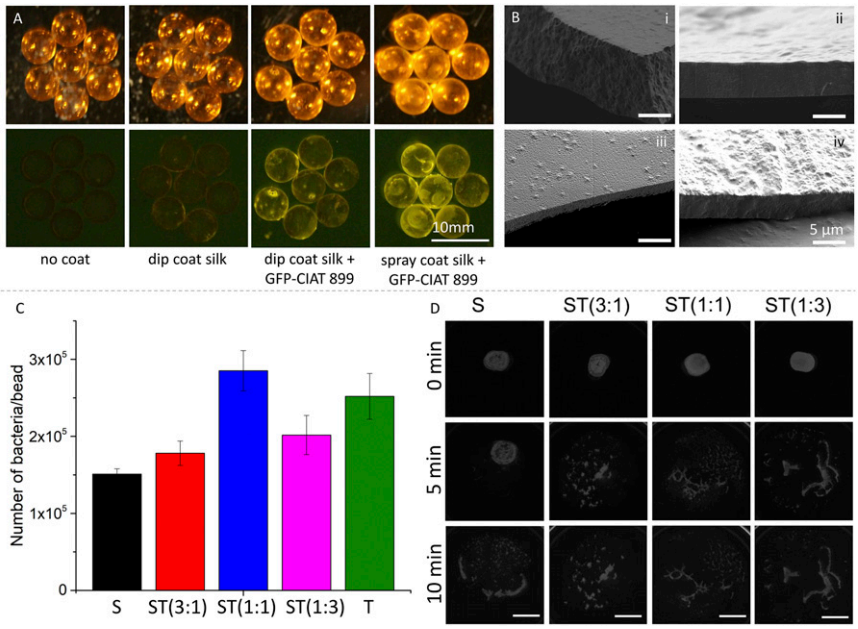

Fig. 2. Coating manufacturing, inoculant encapsulation, and material degradation. (*A*) Single-pot coating of glass beads used as seed phantoms with dip-coating and spray drying techniques. Green fluorescent protein (GFP)-modified CIAT 899 allowed to visualize bacteria distribution on the glass beads. (*B*) Scanning electron microscopy (SEM) micrographs depicting the cross section of (i) silk (S), (ii) ST 3:1 ST(3:1), (iii) ST(1:1), and (iv) ST(1:3) coatings obtained by dip coating. The resulting film thickness was circa 5 µm. The 4 micrographs have been taken at the same magnification. (*C*) Investigation of bacteria encapsulation efficacy during the dip-coating process. The quantity of bacteria per bead after dip coating was quantified by colony counting. All coating solutions had similar dry matter concentration, number of bacteria, and viscosity. Error bars indicate SD. (*D*) Degradation of coating films encapsulating GFP-CIAT 899. Films were positioned on thin phytagels, which were used as transparent artificial soil. Film degradation was investigated as a function of time. Top views of films transilluminated with fluorescence light were taken using a ChemiDoc MP imaging system. (Scale bar is 1 cm.)

number of bacteria encapsulated in the coating (N) by multiplying C_b times the volume of the coating spherical shell (V),

$$N = C_b \cdot V = C_b \cdot \left(\frac{4}{3}\pi R^3 - \frac{4}{3}\pi r^3\right) \approx C_b \cdot (4\pi r^2 t), \qquad [1]$$

where $R = (r + t)$ and $4\pi r^2 t$ is an approximation for the volume of a thin spherical shell obtained as the surface area of the inner sphere multiplied by the thickness t of the shell. Using $r = 0.25$, $t = 0.0005$ cm, and $C_b = 10^{10}/\text{cm}^3$, then $N \approx 3.9{\cdot}10^6$, which indicated a 1 logarithmic reduction of GFP-CIAT 899 culturability during the coating and resuscitation procedures (circa $3{\cdot}10^5$ CIAT 899 were resuscitated from ST coatings as shown in Fig. 2*C*). Using phytagel as a model for soil moisture content, we investigated ST films biodegradation and release of GFP-CIAT 899 using a ChemiDoc MP Imaging System. Time-lapse images of the materials indicated that an increasing relative content of trehalose accelerated material reswelling such that structural integrity was lost within 10 min. Additionally, fluorescence microscopy images taken on glass beads coated with ST materials encapsulating GFP-CIAT 899 showed bacteria release in phytagel a few minutes after materials were in contact with the artificial soil (*SI Appendix*, Fig. S3 and Movie S1).

Preservation of CIAT 899 in ST Coatings. PGPRs, such as CIAT 899, are nonspore forming bacteria with limited viability outside the soil and poor survival postdesiccation (37). Long-term storage of rhizobacteria in seed coatings is one of the major bottlenecks that hinders the large-scale use of these biofertilizers in agricultural practice (38, 39). Application of PGPRs directly in soil and handling of living bacteria require tools and expertise that are not largely available, and thereby the successful encapsulation of PGPRs in seed coatings is seen as a key step to translating the beneficial effects of biofertilizers from bench to field. To assess the potential use of ST materials as seed-coating technology to encapsulate, preserve, and deliver PGPRs, viability and culturability studies were conducted on CIAT 899 embedded in silk, trehalose, and their mixtures at $T = 23$ °C and relative humidity (RH) of 25% and 50% for up to 4 wk. GFP-CIAT 899 preserved in sodium chloride and polymers (e.g., methylcellulose [MC] and polyvinylpyrrolidone [PVP]) found in commercially available seed coatings were used as controls. Fig. 3 shows that ST materials outperformed silk, trehalose, MC, and PVP in preserving GFP-CIAT 899. Interestingly enough, water annealing of silk and ST materials (labeled with A at the end of the sample names in Fig. 3) did not enhance preservation as previously reported for biomolecules, such as antibiotics, enzymes, and growth factors (40, 41), but appeared to be detrimental. S films anneal into a water-insoluble material when left at room temperature and very high RH as the random coil to β-sheet transition is thermodynamically favored (42). This process, commonly named water annealing, causes a partial rehydration and a second drying of the materials which may have stressed and damaged GFP-CIAT899. Viability measurements (Fig. 3, *Top* row) obtained with alamarBlue staining showed that ST(1:3) provided the best environment for GFP-CIAT 899 preservation at both RH levels considered. At week 4 post film formation, more than 25% of GFP-CIAT 899 encapsulated in ST(1:3) films were found to be metabolically active when preserved at RH = 25%. Higher humidity levels decreased viability to ∼5% at week 4, indicating that the coating performance suffers from the hygroscopic nature of the materials used. AlamarBlue was indicative of GFP-CIAT 899 bacteria that were alive (i.e., active metabolic state and intact membrane) postresuscitation. However, in order to survive in a competitive environment, such as the rhizosphere and to form nodules with the host plants, PGPRs need to be able to form colonies. GFP-CIAT 899 reculturability was investigated by streaking resuscitated bacteria on agar plates as a function of storage material,

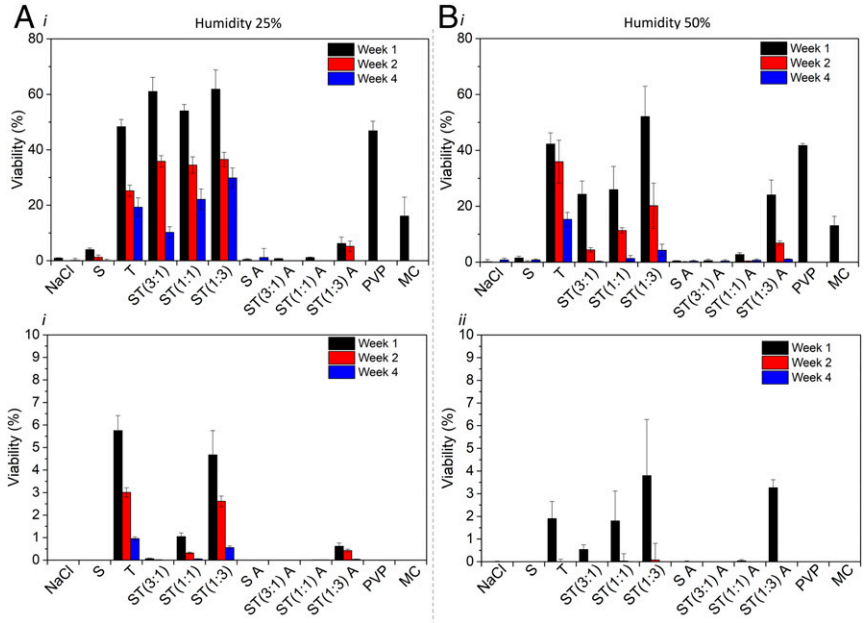

Fig. 3. Preservation of CIAT 899 in silk, trehalose, and their mixtures. Data were collected at weeks 1, 2, and 4 for samples stored at 23 °C and at (*A*) 25% (*B*) 50% RH. In the *Top*, viability indicates the percentage of bacteria that were metabolically active and had intact membranes as investigated by alamarBlue analysis. In the *Bottom*, viability was measured as the percentage of bacteria that were culturable into colonies (colony counting analysis). Data are a pooled average ±SD of $n = 5$ replicates across 10 samples, and a single factor Anova test was used. Silk (S), trehalose (T), ST, x:x indicates the relative weight ratio between the 2 biopolymers, annealed 6 h (A), methyl cellulose (MC), and polyvinylpyrrolidone (PVP).

time, and RH (Fig. 3, *Bottom* row and *SI Appendix*, Figs. S4 and S5). Culture media was not added to resuscitate bacteria in order to better simulate soil conditions where no recovery time would occur. GFP-CIAT 899 colony counting indicated lower viability levels when compared to results obtained with alamarBlue metabolic activity assay, suggesting that a large quantity of GFP-CIAT 899 was viable but nonculturable (VBNC). The VBNC state in PGPRs was previously described as a side effect of desiccation using several encapsulation matrices, including nitrocellulose filters where viability dropped to 4.0% after 1 wk and to less than 2% after 4 wk at RH = 22% (43). In our experiments, silk, trehalose, and ST mixtures produced a statistically significant increase in viability relative to PVP and MC, which are commercially used in seed-coating formulations. Additionally, ST(1:3) preserved GFP-CIAT 899 better than other ST mixtures and with similar performance to pure trehalose, indicating that the disaccharide is the key ingredient in the ST mixture to achieve bacterial reculturability postdesiccation. ST(1:3) was then chosen as the best performing coating because it integrates beneficial trehalose vitrification with the ability of S to provide sufficient mechanical robustness, adhesion, and controllable degradation to the end material. Annealing of S at the point of material fabrication may also be used in the future to control (in a time-dependent manner) the coating biodegradation and consequent release of PGPRs in the surrounding environment.

Intrinsic vs. Extrinsic Trehalose. Several rhizobium species, such as *Rhizobium Etli* are reported to synthesize, uptake, and degrade trehalose (44). The disaccharide accumulates in the cells as an osmoprotectant in response to increasing osmotic pressure of the medium through the otsAB, treS, and treZY synthetic pathways while internal translocation is regulated by permease proteins, such as a trehalose–maltose ABC transporter, encoded by the trehalose transport and utilization (*thu*) operon (*thuEFGK*) (44). For CIAT 899, it has been reported that trehalose synthesis is osmoregulated (45), suggesting the involvement of trehalose in the osmotolerance of this strain. However, it is still unknown if CIAT 899 has ABC transporter proteins capable of translocating trehalose as only evidence for a sorbitol/mannitol ABC transporter have been reported (45). To further investigate the mechanism that underpins stabilization of CIAT 899 in ST materials, we measured intrinsic trehalose content for CIAT 899 incubated in a 1 dry wt% trehalose solution and a 0.09 dry wt% NaCl solution for 1 h. The 1-h time point was used to mimic the amount of time CIAT 899 is in contact with ST materials during solution handling and coating formation. The study showed that, within 1 h, the CIAT 899 intrinsic trehalose concentration was not affected by extrinsic trehalose present in the forming ST materials (Fig. 4*A*). This finding suggests that the stabilization process induced by ST coatings leverages extracellular phenomena, such as vitrification rather than being driven by intracellular translocation of trehalose to provide intrinsic osmotic protection. To further investigate the interplay between extrinsic and intrinsic trehalose in

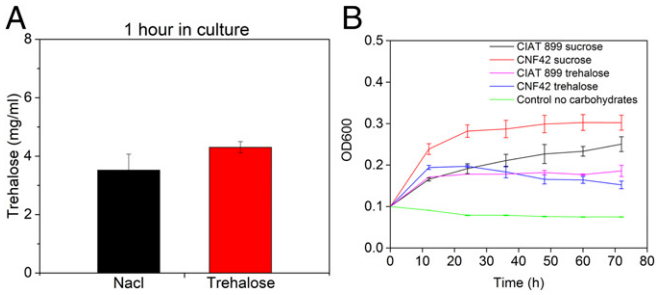

Fig. 4. Interplay between trehalose and CIAT 899. (*A*) Bacteria were cultured for 1 h in 1% dry wt% trehalose solution to measure cellular uptake of extrinsic trehalose. Intrinsic levels of the disaccharide were found to be not statistically significantly different ($P > 0.05$) when compared to the control (0.09 dry wt% NaCl solution). Data are a pooled average ±SD of $n = 7$, and a single factor Anova test was used. (*B*) CIAT 899 and CNF42 were cultured in 0.4% minimal sucrose solution and 0.4% minimal trehalose solution. Growth profiles of CIAT 899 show the ability to translocate and metabolize trehalose and to use it as a carbon source. Data are a pooled average ±SD of $n = 7$.

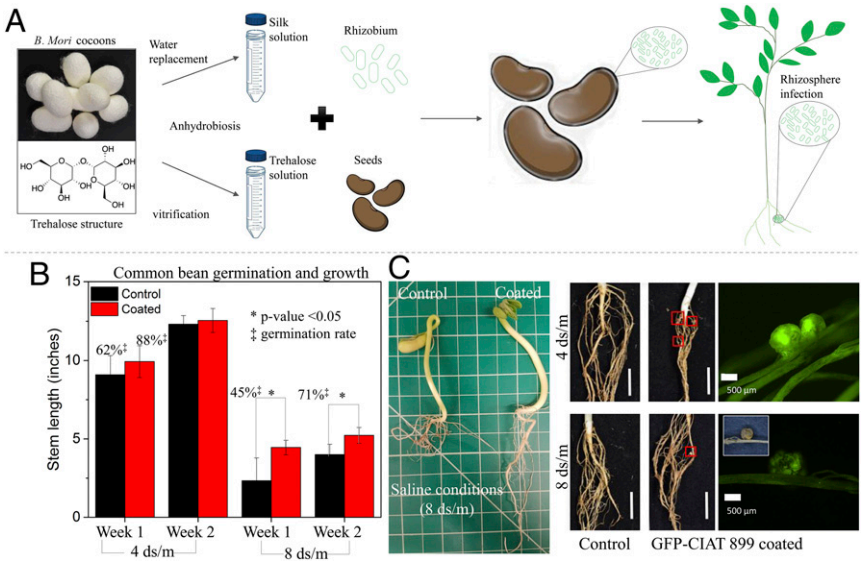

Fig. 5. Seed coating, plant root colonization, and mitigation of saline soil environment. (*A*) Schematic of the strategy used to preserve and deliver CIAT 899 to induce root infections through inoculation by seed coating of common beans. (*B*) Germination rate and stem growth over a 2-wk period in nonsaline (4-ds/m) and saline (8-ds/m) conditions. Error bars indicate SD. (*C*) Macroscopic pictures and fluorescence microscope images of root nodulation confirmed root colonization by GFP-CIAT 899. (Scale bar in root images is 1 cm.) *P. vulgaris* planted per condition, $n = 12$.

CIAT 899, we measured the ability to translocate and metabolize trehalose when compared to a rhizobium strain as *R. etli* CNF42, which is well known to possess the thu operon that can translocate and utilize trehalose (Fig. 4*B*) (46). The study was conducted by culturing CIAT 899 and CNF42 in minimal media using trehalose as a carbon source and sucrose as a positive control. Optical measurements (OD600) showed that CIAT 899 could proliferate in trehalose minimal media as well as CNF42, indicating the ability of CIAT899 to translocate and metabolize trehalose and suggesting that, in the future, longer preexposure to trehalose may lead to enhance preservation performance.

***P. vulgaris* Germination Boost and Mitigation of Saline Soil Conditions.** *P. vulgaris* seeds were dip coated with ST(1:3) encapsulating CIAT 899, dried, and stored for 24 h before planting (Fig. 5*A*). Dip coating was used as it is a cheap, high throughput, and low technology method easily accessible to all farmers (47). Among all of the materials investigated, the ST(1:3) mixture ratio was used given its superior performance in terms of mechanical properties, solution viscosity, and CIAT 899 preservation. Coating processing was designed to coat each seed with 10^7 CIAT 899 bacteria, following requirements generally imposed by policy makers for biofertilizers (48). CIAT 899-coated *P. vulgaris* were grown over a 2-wk period of time in saline (8-ds/m) and nonsaline (4-ds/m) soil using ST(1:3)-coated seeds with no CIAT 899 as the control. Saline soil was established by adding NaCl to topsoil. The CIAT 899-coated *P. vulgaris* seeds exhibited a statistically significant improvement in germination rate for 4- and 8-ds/m soils in comparison to the control seeds. Over the 2-wk investigation period, CIAT 899-coated *P. vulgaris* seeds grew into seedlings that were taller and possessed longer and more articulated roots in comparison to the control seeds (Fig. 5*B*). Visual inspection and fluorescence microscopy were used to assess nodule formation. The right panel of Fig. 5*B* depicts how the GFP-CIAT 899-coated *P. vulgaris* seeds germinated into plants that were colonized by GFP-CIAT 899 as indicated by the presence of nodules that exhibited a strong GFP fluorescence. Interestingly enough, the effectiveness of the CIAT 899-ST (1:3) coating in boosting seed germination and producing stronger seedlings was more evident in the high-salinity 8-ds/m soil.

Conclusion

To summarize, we developed a biomaterial formulation capable of precisely coating seeds with biofertilizers and releasing them in the soil to boost seed germination and mitigate soil salinity. The bioinspired approach that we describe combines a disaccharide well known for its key role in anhydrobiosis with a structural protein that imparts mechanical robustness, ease of fabrication, adhesiveness, conformability, and controlled biodegradation. The rhizobium strain used in this paper survived encapsulation in the biomaterial coating, was preserved over time, and was successfully released in the soil to form symbiotic nodules with the host roots. ST-coated seeds yielded plants that grew faster and stronger in the presence of saline soil. More broadly, our study opens the door to the application of advanced materials to precision agriculture, introducing concepts that are germane to drug delivery and biomaterials design to a field that needs to implement innovative technologies to enhance food production while minimizing inputs and mitigating environmental impacts. Using this approach, it is now possible to define applications where biomaterials can be used to engineer the seed microenvironment to precisely deliver nutrients, hormones, and beneficial biomolecules to seedlings, paving the way for a more sustainable and effective delivery of fertilizers and pesticides.

Data Availability Statement. All data discussed in the paper will be made available to readers upon request to B.M.

ACKNOWLEDGMENTS. We thank Jaime Cheah from MIT Koch Institute for Integrative Cancer Research for helpful technical assistance and discussions; Miguel Lara for GFP *R. tropici* CIAT 899 from Universidad Nacional Autonoma de Mexico. This work was partially supported by the MIT Paul M. Career Professorship, Office of the Dean for Graduate Fellowship, Research Assistantship Fellowship, Office of Naval Research Young Investigator Program (Award N000141812258), and Université Mohammed VI Polytechnique-MIT Research Program.

1. FAO, IFAD, UNICEF, WFP, WHO, *The state of food security and nutrition in the world 2019: Safeguarding against economic slowdowns and downturns* (FAO, Rome, 2019).
2. H. C. J. Godfray *et al.*, Food security: The challenge of feeding 9 billion people. *Science* **327**, 812–818 (2010).
3. R. Gebbers, V. I. Adamchuk, Precision agriculture and food security. *Science* **327**, 828–831 (2010).
4. T. Gomiero, Soil degradation, land scarcity and food security: Reviewing a complex challenge. *Sustainability* **8**, 1–41 (2016).

5. S. Pedrini, D. J. Merritt, J. Stevens, K. Dixon, Seed coating: Science or marketing spin? *Trends Plant Sci.* **22**, 106–116 (2017).
6. L. O. Copeland, M. McDonald, *Principles of Seed Science and Technology* (Springer, US, ed. 4, 2001).
7. A. G. Taylor *et al*., Seed enhancements. *Seed Sci. Res.* **8**, 245–256 (1998).
8. R. Deaker, R. J. Roughley, I. R. Kennedy, Legume seed inoculation technology—A review. *Soil Biol. Biochem.* **36**, 1275–1288 (2004).
9. B. Lugtenberg, F. Kamilova, Plant-growth-promoting rhizobacteria. *Annu. Rev. Microbiol.* **63**, 541–556 (2009).
10. J. K. Vessey, Plant growth promoting rhizobacteria as biofertilizers. *Plant Soil* **255**, 571–586 (2003).
11. D. Bulgarelli, K. Schlaeppi, S. Spaepen, E. Ver Loren van Themaat, P. Schulze-Lefert, Structure and functions of the bacterial microbiota of plants. *Annu. Rev. Plant Biol.* **64**, 807–838 (2013).
12. M. O'Callaghan, Microbial inoculation of seed for improved crop performance: Issues and opportunities. *Appl. Microbiol. Biotechnol.* **100**, 5729–5746 (2016).
13. C. Holland, K. Numata, J. Rnjak-Kovacina, F. P. Seib, The biomedical use of silk: Past, present, future. *Adv. Healthc. Mater.* **8**, e1800465 (2019).
14. Z. Zhou *et al*., Engineering the future of silk materials through advanced manufacturing. *Adv. Mater.* **30**, e1706983 (2018).
15. D. N. Rockwood *et al*., Materials fabrication from Bombyx mori silk fibroin. *Nat. Protoc.* **6**, 1612–1631 (2011).
16. P. Tseng *et al*., Directed assembly of bio-inspired hierarchical materials with controlled nanofibrillar architectures. *Nat. Nanotechnol.* **12**, 474–480 (2017).
17. A. Matsumoto, A. Lindsay, B. Abedian, D. L. Kaplan, Silk fibroin solution properties related to assembly and structure. *Macromol. Biosci.* **8**, 1006–1018 (2008).
18. B. Marelli, M. A. Brenckle, D. L. Kaplan, F. G. Omenetto, Silk fibroin as edible coating for perishable food preservation. *Sci. Rep.* **6**, 25263 (2016).
19. F. G. Omenetto, D. L. Kaplan, New opportunities for an ancient material. *Science* **329**, 528–531 (2010).
20. H.-J. Jin, D. L. Kaplan, Mechanism of silk processing in insects and spiders. *Nature* **424**, 1057–1061 (2003).
21. E. M. Pritchard, D. L. Kaplan, Silk fibroin biomaterials for controlled release drug delivery. *Expert Opin. Drug Deliv.* **8**, 797–811 (2011).
22. J. H. Crowe, F. A. Hoekstra, L. M. Crowe, Anhydrobiosis. *Annu. Rev. Physiol.* **54**, 579–599 (1992).
23. S. Ohtake, Y. J. Wang, Trehalose: Current use and future applications. *J. Pharm. Sci.* **100**, 2020–2053 (2011).
24. J. H. Crowe, J. F. Carpenter, L. M. Crowe, The role of vitrification in anhydrobiosis. *Annu. Rev. Physiol.* **60**, 73–103 (1998).
25. J. H. Crowe, L. M. Crowe, D. Chapman, Preservation of membranes in anhydrobiotic organisms: The role of trehalose. *Science* **223**, 701–703 (1984).
26. N. K. Jain, I. Roy, Effect of trehalose on protein structure. *Protein Sci.* **18**, 24–36 (2009).
27. T. C. Boothby *et al*., Tardigrades use intrinsically disordered proteins to survive desiccation. *Mol. Cell* **65**, 975–984.e5 (2017).
28. A. B. Li, J. A. Kluge, N. A. Guziewicz, F. G. Omenetto, D. L. Kaplan, Silk-based stabilization of biomacromolecules. *J. Control. Release* **219**, 416–430 (2015).
29. N. J. Greenfield, Using circular dichroism spectra to estimate protein secondary structure. *Nat. Protoc.* **1**, 2876–2890 (2006).
30. X. Hu, D. Kaplan, P. Cebe, Determining beta-sheet crystallinity in fibrous proteins by thermal analysis and infrared spectroscopy. *Macromolecules* **39**, 6161–6170 (2006).
31. A. Lerbret, P. Bordat, F. Affouard, M. Descamps, F. Migliardo, How homogeneous are the trehalose, maltose, and sucrose water solutions? An insight from molecular dynamics simulations. *J. Phys. Chem. B* **109**, 11046–11057 (2005).
32. S. H. Williams, B. W. Wright, Vd. Truong, C. R. Daubert, C. J. Vinyard, Mechanical properties of foods used in experimental studies of primate masticatory function. *Am. J. Primatol.* **67**, 329–346 (2005).
33. H. Tao *et al*., Inkjet printing of regenerated silk fibroin: From printable forms to printable functions. *Adv. Mater.* **27**, 4273–4279 (2015).
34. E. Martínez-Romero *et al*., Rhizobium tropici, a novel species nodulating Phaseolus vulgaris L. beans and Leucaena sp. trees. *Int. J. Syst. Bacteriol.* **41**, 417–426 (1991).
35. M. Hungria *et al*., Isolation and characterization of new efficient and competitive bean (Phaseolus vulgaris L.) rhizobia from Brazil. *Soil Biol. Biochem.* **32**, 1515–1528 (2000).
36. M. Hungria, R. J. Campo, I. C. Mendes, Benefits of inoculation of the common bean (Phaseolus vulgaris) crop with efficient and competitive Rhizobium tropici strains. *Biol. Fertil. Soils* **39**, 88–93 (2003).
37. J. A. C. Vriezen, F. J. de Bruijn, K. Nüsslein, Responses of rhizobia to desiccation in relation to osmotic stress, oxygen, and temperature. *Appl. Environ. Microbiol.* **73**, 3451–3459 (2007).
38. A. Zaidi, E. Ahmad, M. S. Khan, S. Saif, A. Rizvi, Role of plant growth promoting rhizobacteria in sustainable production of vegetables: Current perspective. *Sci. Hortic.* **193**, 231–239 (2015).
39. S. B. Sharma, R. Z. Sayyed, M. H. Trivedi, T. A. Gobi, Phosphate solubilizing microbes: Sustainable approach for managing phosphorus deficiency in agricultural soils. *Springerplus* **2**, 587 (2013).
40. J. A. Kluge *et al*., Silk-based blood stabilization for diagnostics. *Proc. Natl. Acad. Sci. U.S.A.* **113**, 5892–5897 (2016).
41. E. Wenk, H. P. Merkle, L. Meinel, Silk fibroin as a vehicle for drug delivery applications. *J. Control. Release* **150**, 128–141 (2011).
42. X. Hu *et al*., Regulation of silk material structure by temperature-controlled water vapor annealing. *Biomacromolecules* **12**, 1686–1696 (2011).
43. J. A. Vriezen, F. J. de Bruijn, K. R. Nüsslein, Desiccation induces viable but Non-Culturable cells in Sinorhizobium meliloti 1021. *AMB Express* **2**, 6 (2012).
44. M. Reina-Bueno *et al*., Role of trehalose in heat and desiccation tolerance in the soil bacterium Rhizobium etli. *BMC Microbiol.* **12**, 207 (2012).
45. C. Fernandez-Aunión *et al*., Biosynthesis of compatible solutes in rhizobial strains isolated from Phaseolus vulgaris nodules in Tunisian fields. *BMC Microbiol.* **10**, 192 (2010).
46. O. Y. Ampomah *et al*., The thuEFGKAB operon of rhizobia and agrobacterium tumefaciens codes for transport of trehalose, maltitol, and isomers of sucrose and their assimilation through the formation of their 3-keto derivatives. *J. Bacteriol.* **195**, 3797–3807 (2013).
47. E. Malusá, L. Sas-Paszt, J. Ciesielska, Technologies for beneficial microorganisms inocula used as biofertilizers. *ScientificWorldJournal* **2012**, 491206 (2012).
48. E. Malusá, N. Vassilev, A contribution to set a legal framework for biofertilisers. *Appl. Microbiol. Biotechnol.* **98**, 6599–6607 (2014).